Pergamon

Pattern Recognition, Vol. 29, No. 3, pp. 463–470, 1996
Elsevier Science Ltd

0031-3203/96 $15.00 + .00

0031-3203(95)00090-9

A POTENTIAL-BASED APPROACH FOR SHAPE MATCHING AND RECOGNITION

JEN-HUI CHUANG

† Department of Computer and Information Science, National Chiao Tung University, Hsinchu, Taiwan 30050, Republic of China

(*Received* 9 *December* 1994; *in revised form* 26 *May* 1995; *received for publication* 28 *June* 1995)

Abstract—This paper presents a novel potential-based approach for recognizing the shape of a two-dimensional (2D) region by identifying the best match from a selected group of shape templates. The proposed model assumes that the border of every 2D region is uniformly charged. An initially small shape template placed inside a shape sample will experience the repulsive force and torque arising from the potential field. A better match in the shape between the template and the sample can be obtained if the template translates and reorients itself to reduce the potential while growing in size. The shape template with the largest final size corresponds to the best match and represents the shape of the given sample. The potential and the associated repulsive force and torque between the polygonal contours are analytically tractable, hence resulting in high computational efficiency of the matching process. The proposed approach is intrinsically invariant under translation, rotation and size changes of the shape sample. Moreover, not only can the matching be carried out directly for shape contours at different viewscales, but the contours can also be unconnected, provided that the template is confined within the shape sample throughout the matching process.

Shape orientation Shape-matching Pattern recognition Artificial potential field

1. INTRODUCTION

One of the major problems in computer vision is object recognition. Many existing algorithms simplify the problem by reducing it to a shape matching and recognition problem. Template matching methods are presented in references (1–3) for object recognition. Fourier descriptors[4,5] transform the coordinates of boundary points into a set of complex numbers for the matching. Moments of 1D functions representing segments of shape contours are used in the matching in references (6–9). Stochastic models, e.g. autoregressive models, are used for shape classification in references (10–12). In references (13–15), the boundary of a region is represented by a sequence of numbers and the shape matching is accomplished by string matching. Other shape matching methods involve finding the polar transform of the shape sample[16] or calculating the distances of the feature points from the centroid,[17] etc. In reference (18) the shape matching is accomplished by graph matching for multilevel structural descriptions of shape samples. Multiple 1D matching processes for multiscale curvature descriptions are adopted in reference (19) in building shape models. Usually, the scaling of the object, the viewscale of the shape contour, the rotation and the translation of the object need to be determined before a final matching process can take place. The matching process may involve the matching of binary images, discrete 1D data, or extracted shape features arranged into structured data.

In this paper, a potential-based approach for shape matching is proposed. The matching process involves the minimization of a scalar function, the potential. The proposed potential model assumes that the border of any 2D region is uniformly charged. If a shape template is small in size and can be placed inside a region whose shape is to be determined, the template will experience repulsive force and torque arising from the potential field. The basic idea of the approach is to achieve a better match in the shape between the template and the given region by translating and reorienting the template along the above force and torque directions, respectively, toward the configuration of the lowest potential. The template is expanded and its position re-adjusted until the template almost touches the border of the given region. For a selected group of shape templates, the template with the largest final size is considered the best match. The proposed approach is intrinsically invariant under translation, rotation and size changes of the shape sample. The location, orientation and the scaling of the object can then be obtained as side products of the shape recognition. Moreover, not only can the matching be carried out directly for shape contours at different viewscales without resorting to multiscale matching, but the contours

Part of this work was presented at the 1993 Asian Conference on Computer Vision. This work was supported by National Science Council, Republic of China, under NSC-82-0408-E009-283.

can also be unconnected provided that the template remains inside the shape sample throughout the matching process.

The Newtonian potential model is adopted in this paper, wherein the potential is inversely proportional to the distance between any two point charges. In the aforementioned shape matching process, the main computation associated with the minimization of the potential is the calculation of the repulsive force and torque between the shape contours. These potential-related quantities can be derived analytically for such a potential model, avoiding the expensive numeric implementation of the discretization of the shape contours before calculating the repulsive force and torque. Therefore, the proposed potential-based shape matching can achieve a high efficiency.

The potential function due to the repulsion between two uniformly charged region boundaries is derived in Section 2. Section 3 presents the derivation of the analytic expressions for the repulsive force and torque. The computer implementation, including a graphic user interface, is presented in Section 4 along with some simulation results. Section 5 presents concluding remarks.

2. THE POTENTIAL FUNCTION

Consider a point A located at $(0, y_0)$ and a finite line charge on the x axis with a unit charge density uniformly distributed between $x = x_1$ and $x = x_2$, as shown in Fig. 1. The Newtonian potential at point A due to a point $(x, 0)$ of the line charge is:

$$\frac{1}{r} = \frac{1}{\sqrt{x^2 + y_0^2}}, \quad x_1 \le x \le x_2. \tag{1}$$

where r is the distance between these two points. The total potential at point A due to the whole line segment can then be calculated as:

$$\phi_A = \int_{x_1}^{x_2} \frac{dx}{r} = \int_{x_1}^{x_2} \frac{dx}{\sqrt{x^2 + y_0^2}} = \log \frac{|x_2 + \sqrt{x_2^2 + y_0^2}|}{|x_1 + \sqrt{x_1^2 + y_0^2}|}. \tag{2}$$

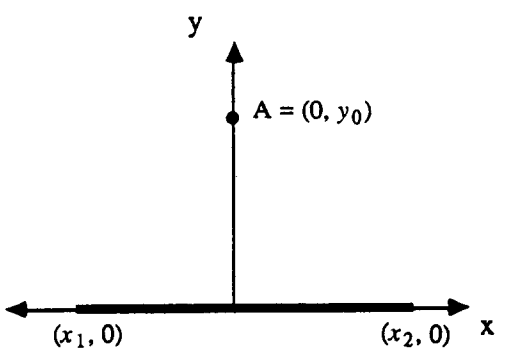

Fig. 1. A finite line charge and a point A in a selected coordinate system.

In the general case, let **a** and **b** be the end points of a line segment $\overline{ab}$ and **c** the point for which the Newtonian potential is to be calculated. Assume that the vector $\mathbf{v}_{ab} \triangleq \mathbf{b} - \mathbf{a}$ stays on the x axis and is directed to the right. Also assume that the points **a**, **b** and **c** do not stay on the same line. It can be shown that (2) is still valid with:

$$x_1 = \hat{\pi}_{ab} \cdot \mathbf{v}_{ca}. \tag{3}$$

$$x_2 = \hat{\pi}_{ab} \cdot \mathbf{v}_{cb}. \tag{4}$$

$$y_0 = \mathbf{v}_{ac} \cdot \hat{\pi}_{ab}^{+}, \tag{5}$$

where $\mathbf{v}_{ca} \triangleq \mathbf{a} - \mathbf{c}$, $\mathbf{v}_{cb} \triangleq \mathbf{b} - \mathbf{c}$, $\hat{\pi}_{ab}$ is the unit vector in the $\mathbf{v}_{ab}$ direction and $\hat{\pi}_{ab}^{+}$ is a unit vector perpendicular to $\hat{\pi}_{ab}$ with $\hat{\pi}_{ab} \times \hat{\pi}_{ab}^{+}$ in the $+z$ direction.

In order to calculate the potential due to the repulsion between polygonal regions, we need to calculate the potential due to the repulsion between two line segments. The potential due to the repulsion between the polygonal regions (Section 2.1) can then be obtained according to the superposition principle.

2.1. *Potential due to repulsion between polygonal regions*

Consider the two line segments $\overline{ab}$ and $\overline{cd}$ shown in Fig. 2. The coordinates of the end points **a**, **b**, **c** and **d** are assumed to be (a_1, a_2), (b_1, b_2), $(0, 0)$ and $(d_1 \ge 0, 0)$, respectively (after a coordinate transformation). Let:

$$\hat{\pi}_{ab} \triangleq (n_1, n_2), \tag{6}$$

be the unit vector along the $\mathbf{v}_{ab}$ direction, equations (3), (4) and (5) for an object point on $\overline{cd}$, say $\mathbf{x} = (x, 0)$, become:

$$x_1(x) = (a_1 - x)n_1 + a_2 n_2 \triangleq kx + l, \tag{7}$$

$$x_2(x) = (b_1 - x)n_1 + b_2 n_2 \triangleq ix + j, \tag{8}$$

and

$$y_0(x) = -(x - a_1)n_2 + (-a_2)n_1 \triangleq gx + h, \tag{9}$$

respectively.

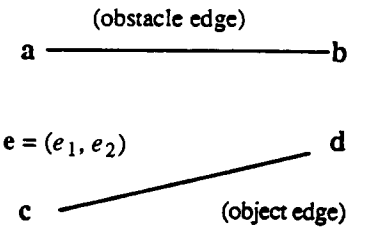

Fig. 2. Two line segments and a reference point for the calculation of the repulsive force and torque due to the Newtonian potential.

If both $\overline{ab}$ and $\overline{cd}$ are uniformly charged, by substituting equations (7)–(9) into (2), the potential due to the repulsion between $\overline{ab}$ and $\overline{cd}$ is equal to:

$$\int_0^{d_1} \log(ix+j+\sqrt{(ix+j)^2+(gx+h)^2})\,dx - \int_0^{d_1} \log(kx+l+\sqrt{(kx+l)^2+(gx+h)^2})\,dx. \quad (10)$$

With a proper change of variables, the integrals can be simplified into the following form which can be evaluated analytically:

$$\int \log(x+\sqrt{x^2+(ax+b)^2})\,dx = -x+\frac{2b\log|ax+b|}{a}+x\log(x+\sqrt{x^2+(ax+b)^2}) - \frac{b\log|-a^2x+a^2\sqrt{x^2+(ax+b)^2}|}{a} - \frac{b\log|ab+c^2x+c\sqrt{x^2+(ax+b)^2}|}{ac^2}, \quad (11)$$

where a and b are constants and

$$c \triangleq \sqrt{1+a^2}. \quad (12)$$

Therefore, the repulsive potential between two polygonal regions can be obtained in closed form by superposing the repulsive potential calculated analytically using (11) for every pair of linear segments obtained from the two different region borders.

Figure 3 shows the potential profiles obtained for three different sizes of a square template rotating 360° inside a square region. As the size increases, the potential valleys become much easier to be identified for the template that matches the square region perfectly. Figure 4 shows the potential profiles obtained for (a) equilateral triangular, (b) rectangular and (c) square templates, all having the same area, rotating 360° inside a square region. It is clear that the potential profile for the triangular template always has a much higher value than the potentials for the square tem-

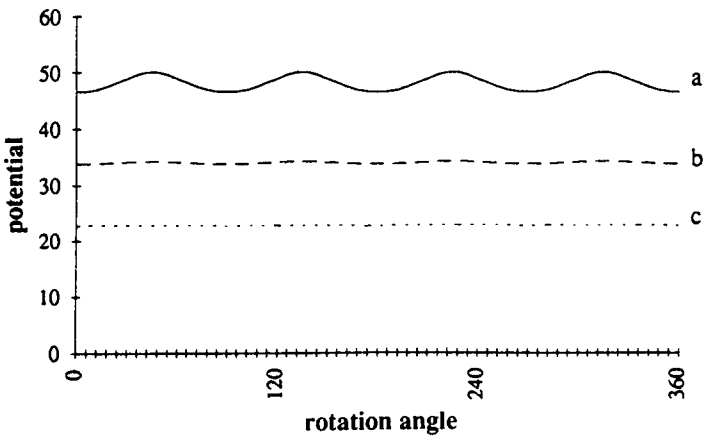

Fig. 3. The potential profiles obtained for different sizes of a square template rotating 360 degrees inside a square region. The template has (a) 49%, (b) 30%, and (c) 15% of the area of the region, respectively.

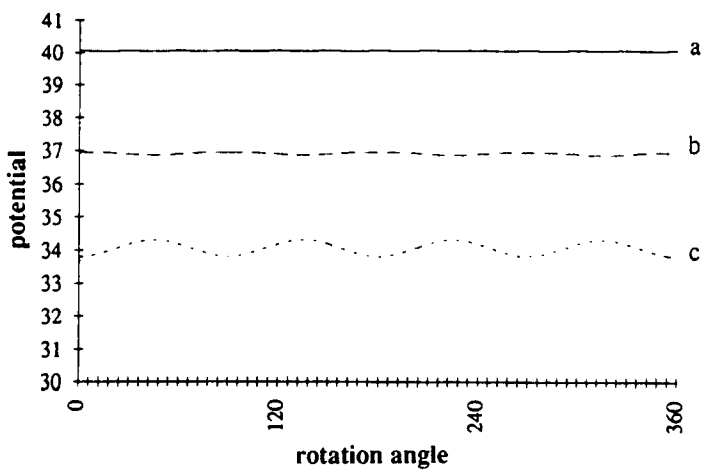

Fig. 4. The potential profiles obtained for (a) regular triangular, (b) rectangular, and (c) square template rotating 360 degrees inside a square region. All templates are of the same area, 30% of that of the square region.

plate that yields the best match. Moreover, the potential valleys are clearly observable and can be identified easily, only for the square template.

With the above analytic expressions for the repulsive potential between polygonal boundaries, the numerical evaluation of repulsion, which requires discretization of such shape boundaries can be avoided. In fact, the minimizaton of the potential in the shape matching can be performed with a more efficient, gradient-based search if, in addition, the repulsive force and torque can also be expressed in closed forms, as will be discussed in the next section.

3. THE REPULSIVE FORCE AND TORQUE IN CLOSED FORM

The negative gradient of the potential function is the repulsive force experienced by a point charge of unit strength. Moving along the force direction corresponds to a maximal reduction rate of the potential away from that point. The repulsive force on point A in Fig. 1 due to a point $(x,0)$ on the x axis is:

$$-\nabla\left(\frac{1}{r}\right)=\frac{1}{r^2}\hat{\mathbf{r}}=\frac{1}{x^2+y_0^2}(\cos\theta\hat{\mathbf{x}}+\sin\theta\hat{\mathbf{y}}), \quad (13)$$

where θ is the angle between the position vector and the x axis, measured in the counterclockwise direction. Therefore, the resulting force from the line segment on A can be calculated from:

$$F_x=\int_{x_1}^{x_2}\frac{\cos\theta\,dx}{r^2(x)}=\int_{x_1}^{x_2}\frac{-x\,dx}{(x^2+y_0^2)^{3/2}}=\frac{1}{\sqrt{x_2^2+y_0^2}}-\frac{1}{\sqrt{x_1^2+y_0^2}} \quad (14)$$

and

$$F_y=\int_{x_1}^{x_2}\frac{\sin\theta\,dx}{r^2(x)}=\int_{x_1}^{x_2}\frac{y_0\,dx}{(x^2+y_0^2)^{3/2}}=\frac{x_2}{y_0\sqrt{x_2^2+y_0^2}}-\frac{x_1}{y_0\sqrt{x_1^2+y_0^2}}, \quad (15)$$

where F_x is the force component along the x axis and F_y is along the y axis.

Therefore, for the two line segments $\overline{ab}$ and $\overline{cd}$ shown in Fig. 2, the repulsive force on point $(x,0)$ due to the line charge $\overline{ab}$ can be expressed as:

$$\mathbf{F}(x)=F_{ab}(x)\hat{\mathbf{n}}_{ab}+F_{ab}^{+}(x)\hat{\mathbf{n}}_{ab}^{+}, \quad (16)$$

where

$$F_{ab}(x)=\frac{1}{\sqrt{x^2+bx+c}}-\frac{1}{\sqrt{x^2+ex+f}}, \quad (17)$$

$$F_{ab}^{+}(x)=\frac{1}{gx+h}\left(\frac{ix+j}{\sqrt{x^2+bx+c}}-\frac{kx+l}{\sqrt{x^2+ex+f}}\right), \quad (18)$$

and $b, c, e, f, g, h, i, j, k$ and l are constants since x_1, x_2 and y_0 are *linear* functions of x according to equations (9)–(11).

3.1. *The repulsive force and torque between two line segments*

For the two mutually repelling line segments shown in Fig. 2, the resultant repulsive force on $\overline{cd}$ can be calculated with:

$$\mathbf{F}=\int_0^{d_1}\mathbf{F}(x)\,dx, \quad (19)$$

using equations (16)–(18). On the other hand, the torque with respect to an arbitrary point $\mathbf{e}=(e_1,e_2)$ due to the repulsion from $\overline{ab}$ to point $\mathbf{x}=(x,0)$ of $\overline{cd}$ is:

$$\mathbf{T}(x)=\mathbf{F}(x)\times(\mathbf{x}-\mathbf{e}), \quad (20)$$

which is in either the $+z$ or $-z$ direction. Therefore, the total torque in the $+z$ direction due to repulsion between $\overline{ab}$ and $\overline{cd}$ is:

$$T_z=\int_0^{d_1}T_z(x)\,dx. \quad (21)$$

It is not hard to show from equations (19) and (21) that the calculations of the repulsive force and torque require the evaluation of integrals of the following forms:

$$\int\frac{dx}{\sqrt{x^2+bx+c}}=\log\left|\frac{b}{2}+x+\sqrt{x^2+bx+c}\right| \quad (22)$$

$$\int\frac{x\,dx}{\sqrt{x^2+bx+c}}=\sqrt{x^2+bx+c}-\frac{b}{2}\int\frac{dx}{\sqrt{x^2+bx+c}} \quad (23)$$

$$\int\frac{dx}{x\sqrt{x^2+bx+c}}=-\frac{1}{\sqrt{c}}\log\left|\frac{\sqrt{x^2+bx+c}+\sqrt{c}}{x}+\frac{b}{2\sqrt{c}}\right| \quad (24)$$

$$\int\sqrt{x^2+bx+c}\,dx=\frac{2x+b}{4}\sqrt{x^2+bx+c}-\frac{b^2-4c}{8}\int\frac{dx}{\sqrt{x^2+bx+c}}, \quad (25)$$

which are all analytically integrable. (Formulations for special cases, e.g. when $c=0$, are omitted for simplicity.) Thus, the repulsive force and torque can be evaluated in closed forms and the conceptually simple, potential-based shape-matching methods can be implemented efficiently using these analytic results, as will be discussed next.

4. COMPUTER IMPLEMENTATION AND SIMULATION RESULTS

In the computer implementation, a graphic user interface is developed, as shown in Fig. 5. A selected group of shape templates are shown on one side of the screen. Additional templates can be added easily into the database. Each of the templates is initialized to have the same area. The only assumption is that the templates

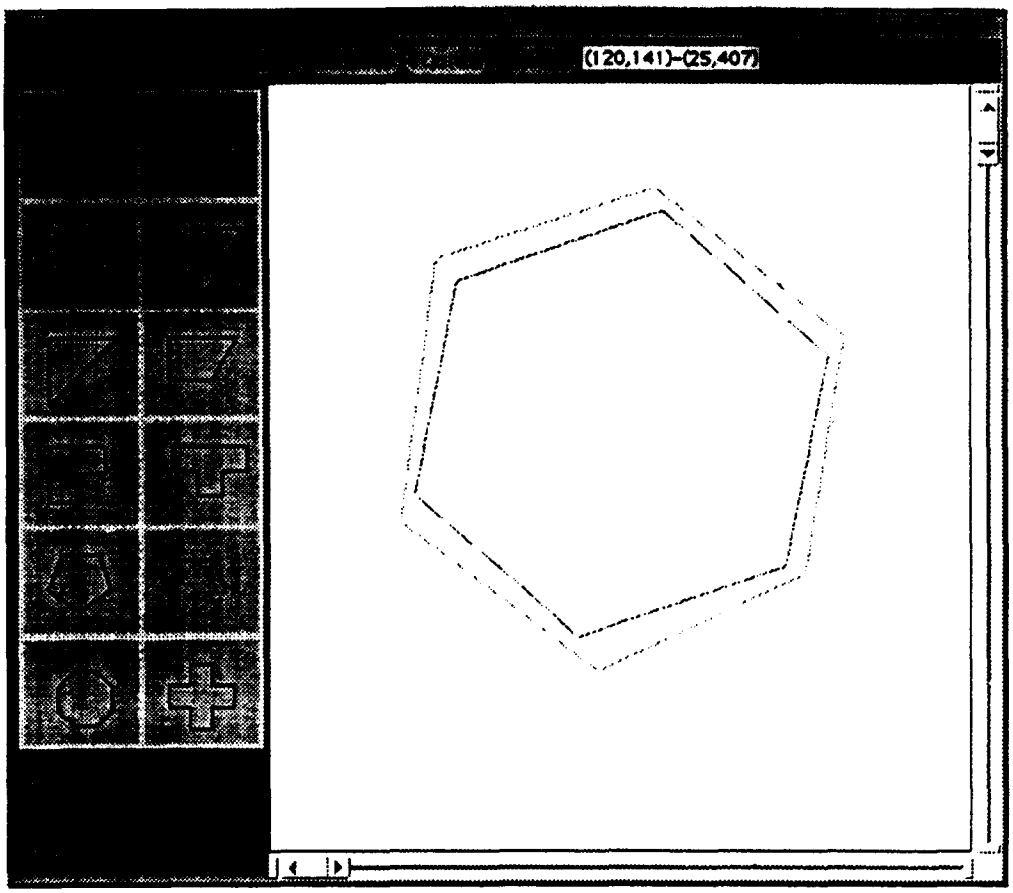

Fig. 5. A simple graphic user interface for shape matching.

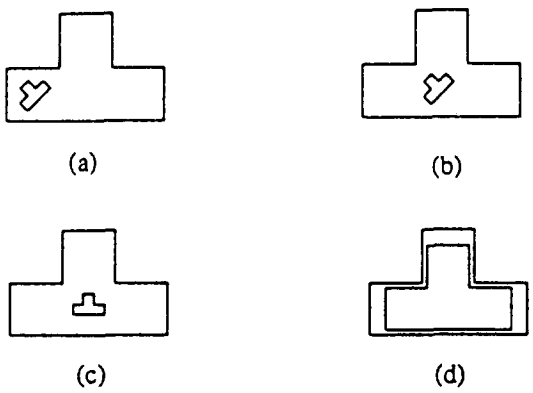

Fig. 6. The basic matching procedure: (a) place a (size-reduced) template inside the input region, (b) translate and (c) rotate the template to reduce the potential, then (d) increase the size of the template.

are small enough initially that each of them can be placed inside the input region whose shape is to be recognized. The region whose shape is to be recognized is scanned, followed by a boundary detection procedure. Precise imformation about the location, orientation and the size of the input region is not needed.

For the shape matching process, the following operations are performed for a shape template placed inside the input region (see Fig. 6):

Step 1. Translate along the force direction derived from equation (19) until the force is negligible.

Step 2. Rotate, with the centroid of the template being the rotation center, along the torque direction derived from equation (21) until the torque is negligible.

Step 3. With the location of the centroid fixed in space, increase the size of the template as much as possible (as long as the template remains inside the region of interest).

Step 4. End if the increase in Step 3 is negligible, otherwise go to Step 1.

The same procedure is executed for each of the shape templates. The shape of the template having the largest area after the above operations is identified as the shape of the input region.

Figure 7 shows the simulation results for four input regions. An ideal case is shown in Fig. 7(a), where a perfect match exists for a T-shaped input region and one of the 12 templates. The matching results shown for each template include (1) the initial template configuration, (2) the template after the matching operations are completed and (3) the input region whose configuration remains unchanged throughout the matching process.

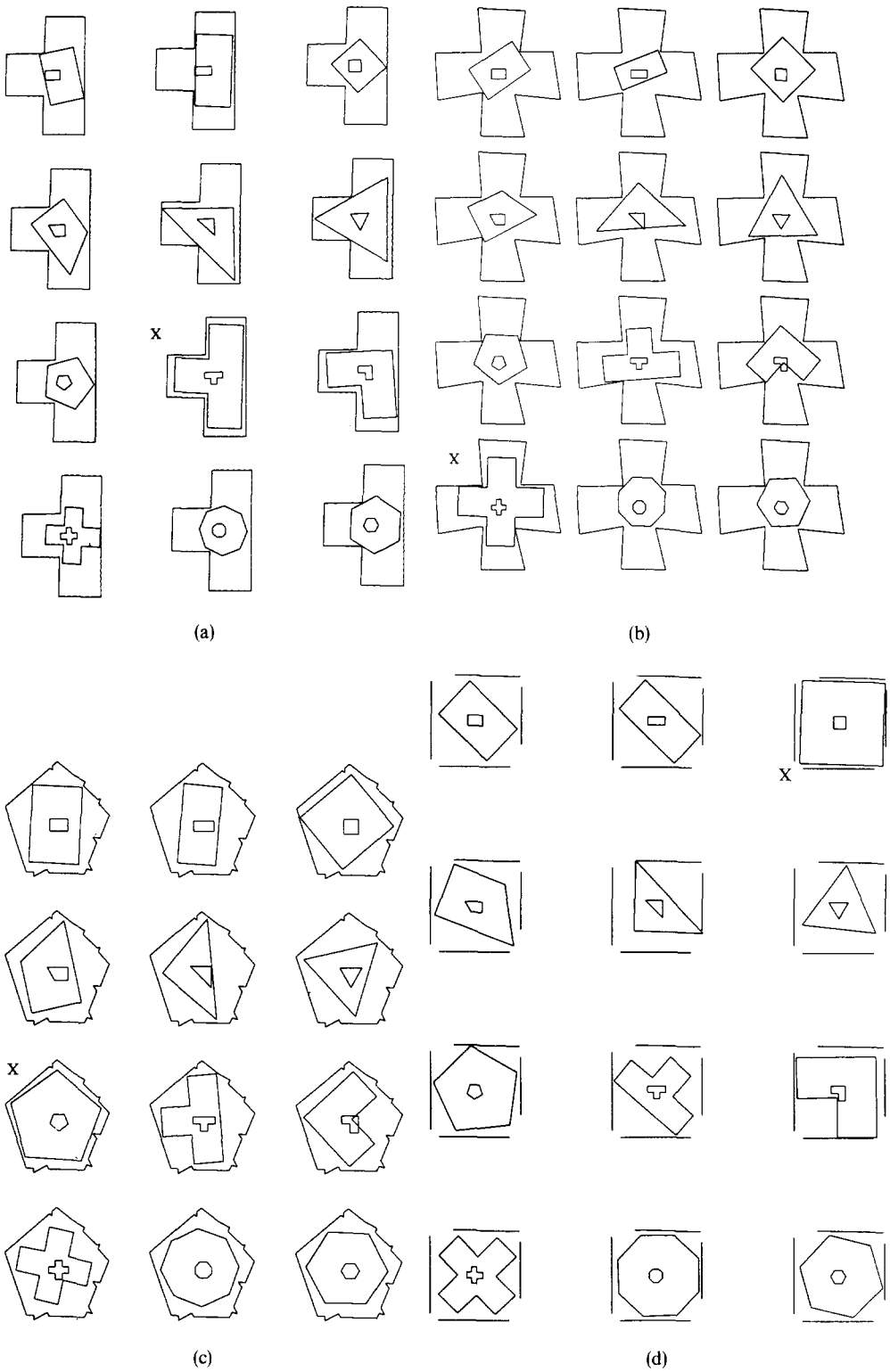

Fig. 7. Shape matching examples, the best match is marked by an "x".

The total simulation time for the complete matching and recognition processes takes less than 10s on a Sun SPARCstation 10. Similar shape-matching results are shown in Fig. 7(b), where the shape of the input region is somewhat distorted from the corresponding template. Figure 7(c) shows a successful match in shape for an input region which has a noisy boundary. In this case, part of the boundaries of the template and the input region are also at different viewscales, i.e. the number of line segments of the boundaries have different orders of

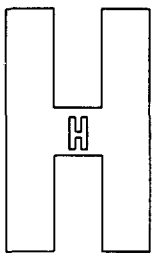

Fig. 8. An H-shaped region and the corresponding shape template.

magnitude. Figure 7(d) shows the matching results for an input region whose border is not connected. The proposed approach will work for such a situation as long as the template, under the influence of the potential, remains confined within the input region throughout the matching process.

Similar to some other shape-matching methods, locally optimal match in shape may be obtained with the proposed approach. The globally best match corresponds to the global minimum of the potential function. Such a match can be found if the simulation is done for several, typically no more than four for the examples presented in this paper, initial rotation angles for each of the templates.

There are cases when the above simple shape-matching process failed to generate correct results. For example, consider the H-shaped input region and the corresponding shape template placed inside that region, shown in Fig. 8. The final size of the template after the size increase operations will be far less than the size of the input region, resulting in a meaningless match. In order to resolve such a problem, more sophisticated size increase operations are needed. For example, instead of using the shape template, its skeleton can be used to represent the shape. The size increase process will then consist of two parts: the growing of the skeleton (which may not be straightforward) followed by the growing of the template from its skeleton.

5. CONCLUSIONS

A potential-based shape-matching and recognition method is presented in this paper. The approach is invariant under translation, rotation and size changes of the input region whose shape is to be recognized. The shape-matching concept is simple, and is implemented efficiently using the analytically derived expressions associated with the potential function. For the template of the best match, it is shown that the global behavior of the variation in potential can be improved by increasing the size of the template during the matching process and that the potential valleys become much easier to identify. Thus, the size of the input region need not be normalized explicitly. The approach can use directly the original boundary description of the input region, which may be at a different viewscale from that of the shape templates. The approach may also work for a region whose boundary is not connected.

6. FUTURE WORK

An extension of the above shape-matching concept will be useful in solving the path planning problems. In order to ensure that a moving object is free from collision with the obstacles, the shape of the object and the shape of the free space should be matched properly along the planned path. For the shape matching discussed in this paper, the size of the shape template is allowed to increase while its location is confined inside the region of unknown shape. For the shape matching in path planning, on the other hand, the size of the object is fixed, and its shape should be matched locally with the free space at different locations along the path. The proposed shape matching concept can be generalized to the 3D space to recognize the shape of 3D objects. This generalization is currently under investigation.

REFERENCES

1. W. A. Perkins, A model based vision system for industrial parts, *IEEE Trans. Comput.* **21**, 126–143 (1978).
2. P. Rummel and W. Beutel, Workpiece recognition and inspection by a model-based scene analysis system, *Pattern Recognition* **17**, 141–148 (1984).
3. N. Ayache and O. D. Faugeras, HYPER: A new approach for the recognition and positioning of two-dimensional objects, *IEEE Trans. Pattern Anal. Mach. Intell.* **8**, 44–54 (1986).
4. C. T. Zahn and R. Z. Roskies, Fourier descriptors for plane closed curves, *IEEE Trans. Comput.* **21**, 269–281 (1972).
5. E. Persoon and K. S. Fu, Shape discrimination using Fourier descriptors, *IEEE Trans. Syst. Man Cybern.* **7**, 170–179 (1977).
6. M. K. Hu, Visual pattern recognition by moment invariants, *IEEE Trans. Inf. Theory* **8**, 179–187 (1962).
7. S. Maitra, Moment invariants, *Proc. IEEE* **67**, 697–699 (1979).
8. S. S. Reddi, Radial and angular moment invariants for image identification, *IEEE Trans. Pattern Anal. Mach. Intell.* **3**, 240–242 (1981).
9. J. G. Leu, Computing a shape's moments from its boundary, *Pattern Recognition* **24**, 949–957 (1991).
10. S. R. Dubois and F. H. Glanz, An autoregressive model approach to two-dimensional shape classification, *IEEE Trans. Pattern Anal. Mach. Intell.* **8**, 55–66 (1977).
11. R. L. Kashyap and R. Chellappa, Stochastic models for close boundary analysis: representation and reconstruction, *IEEE Trans. Inf. Theory* **27**, 627–637 (1981).
12. M. Das, M. J. Paulik and N. K. Loh, A bivariate autoregressive modeling technique for analysis and classification of planar shapes, *IEEE Trans. Pattern Anal. Mach. Intell.* **12**, 97–103 (1990).
13. H. Freeman and L. S. Davis, A corner finding algorithm for chain coded curves, *IEEE Trans. Comput.* **26**, 297–303 (1977).
14. W. H. Tsai and S. S. Yu, Attributed string matching with merging for shape recognition, *IEEE Trans. Pattern Anal. Mach. Intell.* **7**, 453–462 (1985).
15. M. Maes, Polygonal shape recognition using string-matching techniques, *Pattern Recognition* **24**, 433–440 (1991).

16. A. Blumenkrans, two-dimensional object recognition using a two-dimensional polar transform, *Pattern Recognition* **24**, 879–890 (1991).
17. C. C. Chang, S. M. Hwang and D. J. Buehrer, A shape recognition scheme based on relative distances of feature points from the centroid, *Pattern Recognition* **24**, 1053–1063 (1991).
18. L. G. Shapiro and R. M. Haralick, Structural descriptions and inexact matching, *IEEE Trans. Pattern Anal. Mach. Intell.* **3**, 504–519 (1981).
19. N. Ueda and S. Suzuki, Learning visual models from shape contours using multiscale convex/concave structure matching, *IEEE Trans. Pattern Anal. Mach. Intell.* **15**, 337–352 (1993).

About the Author—JEN-HUI CHUANG was born on 27 March 1958 in Taipei, Taiwan, Republic of China. He received the B.S. degree in electrical engineering from National Taiwan University in 1980, the M.S. degree in electrical and computer engineering from the University of California at Santa Barbara in 1983 and the Ph.D. degree in electrical and computer engineering from the University of Illinois at Urbana-Champaign in 1991. Between 1983 and 1985 he was a design and development engineer with LSI Logic Corporation, Milpitas, California. Between 1985 and 1989 he was a research assistant with the Signal Processing Group at the Coordinated Science Laboratory, University of Illinois. Between 1989 and 1991 he was a research assistant with the Robot Vision Laboratory at the Beckman Institute for Advanced Science and Technology, University of Illinois. Since August 1991, he has been on the faculty of the Department of Computer and Information Science at National Chiao Tung University. His research interests include robotics, computer vision, signal and image processing and VLSI systems. Dr Chuang is a member of IEEE and the Tau Beta Pi Society.